Altered grey matter integrity and network vulnerability relate to epilepsy occurrence in patients with multiple sclerosis

Dumitru Ciolac, Gabriel Gonzalez Escamilla, Yaroslav Winter, Nico Melzer, Felix Luessi, Angela Radetz, Vinzenz Fleischer, Stanislav A. Groppa, Michael Kirsch, Stefan Bittner, Frauke Zipp, Muthuraman Muthuraman, Sven G. Meuth, Matthias Grothe, Sergiu Groppa

ORIGINAL ARTICLE

Altered grey matter integrity and network vulnerability relate to epilepsy occurrence in patients with multiple sclerosis

Dumitru Ciolac[1,2,3] | Gabriel Gonzalez-Escamilla[1] | Yaroslav Winter[4,5] |
Nico Melzer[6] | Felix Luessi[1] | Angela Radetz[1] | Vinzenz Fleischer[1] |
Stanislav A. Groppa[2,3] | Michael Kirsch[7] | Stefan Bittner[1] | Frauke Zipp[1] |
Muthuraman Muthuraman[1] | Sven G. Meuth[6] | Matthias Grothe[8] | Sergiu Groppa[1]

[1]Department of Neurology, Focus Program Translational Neuroscience (FTN), Rhine-Main Neuroscience Network (rmn[2]), University Medical Center of the Johannes Gutenberg University Mainz, Mainz, Germany

[2]Nicolae Testemitanu State University of Medicine and Pharmacy, Chisinau, Moldova

[3]Department of Neurology, Institute of Emergency Medicine, Chisinau, Moldova

[4]Mainz Comprehensive Epilepsy and Sleep Medicine Center, Department of Neurology, Johannes Gutenberg University Mainz, Mainz, Germany

[5]Department of Neurology, Philipps-University, Marburg, Germany

[6]Department of Neurology, Heinrich Heine University, Düsseldorf, Germany

[7]Institute for Diagnostic Radiology and Neuroradiology, University Medicine of Greifswald, Greifswald, Germany

[8]Department of Neurology, University Medicine of Greifswald, Greifswald, Germany

Correspondence
Sergiu Groppa, Department of Neurology, Focus Program Translational Neuroscience (FTN), Rhine-Main Neuroscience Network (rmn), University Medical Center of the Johannes Gutenberg University Mainz, Langenbeckstrasse 1, 55131 Mainz, Germany.
Email: segroppa@uni-mainz.de

Funding information
This study was supported by the German Research Foundation (DFG; CRC-TR-128).

Abstract

Background and purpose: The aim of this study was to investigate the relevance of compartmentalized grey matter (GM) pathology and network reorganization in multiple sclerosis (MS) patients with concomitant epilepsy.

Methods: From 3-T magnetic resonance imaging scans of 30 MS patients with epilepsy (MSE group; age 41 ± 15 years, 21 females, disease duration 8 ± 6 years, median Expanded Disability Status Scale [EDSS] score 3), 60 MS patients without epilepsy (MS group; age 41 ± 12 years, 35 females, disease duration 6 ± 4 years, EDSS score 2), and 60 healthy subjects (HS group; age 40 ± 13 years, 27 females) the regional volumes of GM lesions and of cortical, subcortical and hippocampal structures were quantified. Network topology and vulnerability were modelled within the graph theoretical framework. Receiver-operating characteristic (ROC) curve analysis was applied to assess the accuracy of GM pathology measures to discriminate between MSE and MS patients.

Results: Higher lesion volumes within the hippocampus, mesiotemporal cortex and amygdala were detected in the MSE compared to the MS group (all $p < 0.05$). The MSE group had lower cortical volumes mainly in temporal and parietal areas compared to the MS and HS groups (all $p < 0.05$). Lower hippocampal tail and presubiculum volumes were identified in both the MSE and MS groups compared to the HS group (all $p < 0.05$). Network topology in the MSE group was characterized by higher transitivity and assortativity, and higher vulnerability compared to the MS and HS groups (all $p < 0.05$). Hippocampal lesion volume yielded the highest accuracy (area under the ROC curve 0.80 [0.67–0.91]) in discriminating between MSE and MS patients.

Conclusions: High lesion load, altered integrity of mesiotemporal GM structures, and network reorganization are associated with a greater propensity for epilepsy occurrence in people with MS.

KEYWORDS
epilepsy, grey matter integrity, lesion load, multiple sclerosis, network vulnerability

---

Dumitru Ciolac and Gabriel Gonzalez-Escamilla contributed equally to this work.

INTRODUCTION

Seizures and epilepsy may occur during the course of multiple sclerosis (MS). Their prevalence is estimated to be 1.5%–2.6% [1, 2] and 0.9%–3.1% [1], respectively, which is approximately seven times higher than in the general population [3]. The underlying causes of a higher susceptibility to epilepsy occurrence in MS patients are poorly understood, however, an earlier onset of MS, longer disease duration, and greater disability have been suggested as predisposing factors [4]. A few available neuroimaging and neuropathological studies emphasized the specific role of inflammatory and degenerative cortical grey matter (GM) damage [5, 6] in promoting the occurrence of epilepsy in MS. In particular, inflammatory lesions, neuronal cell loss, and axonal demyelination were recognized as driving mechanisms of cortical hyperexcitability and seizure generation in MS [5, 7]. Quantification of both lesion and tissue morphometric properties across different GM compartments might reveal structural abnormalities associated with epileptogenesis due to MS pathology. As spatial location of lesions and cortical atrophy are non-random and follow specific patterns in MS [8], the relationship between regional distribution of GM pathology and epilepsy occurrence is of great interest. Due to the primary attribution of temporal lobe damage in seizure generation in MS patients [5, 9], involvement of other cortical and subcortical structures has remained less well studied.

Inflammatory lesions and tissue loss induce early and widespread brain network responses in MS patients, involving cortical and subcortical GM structures [10–13]. Similarly, network remodelling occurs in epilepsy patients, locally within the seizure focus and spanning towards the distant areas [14–16]. Graph theory is a valuable tool with which to investigate the alterations of brain networks in both MS [17] and epilepsy [18] patients. Network alterations in MS patients with concomitant epilepsy have not been approached so far and addressing these might offer additional insights into the network mechanisms linked to epileptogenesis in MS.

In this study, we aimed to assess the contribution of compartmentalized GM pathology and network architecture to epilepsy occurrence in patients with MS. Hence, we analysed regional T2 lesion loads and volumes of cortical, subcortical and hippocampal GM structures, and modelled GM connectivity matrices in MS patients with and without epilepsy. We hypothesized that MS patients with concomitant epilepsy display specific topographical alterations in GM structures and network organization that favour epilepsy occurrence.

METHODS AND MATERIALS

Study participants

This study was conducted at two neurology centres in Germany: the Department of Neurology at the University Medical Centre of the Johannes Gutenberg University Mainz and the Department of Neurology at the University Medicine Greifswald. From a large MS cohort (n = 1156), 30 patients satisfying the study's criteria, namely, diagnosis of MS based on the 2010 McDonald criteria [19] and concomitant epilepsy not explained by causes other than MS (MSE group), were included. Among these, 25 had relapsing–remitting MS (RRMS), three had secondary progressive MS (SPMS) and two had primary progressive MS (PPMS). Epilepsy was defined as the occurrence of two unprovoked epileptic seizures presenting more than 24 h apart [20] and epilepsy type was classified according to the International League Against Epilepsy (ILAE) criteria [21]. Classification of seizure type into focal, generalized or unknown onset was performed according to the 2017 ILAE guidelines [22]. A control group of 60 age- and sex-matched MS patients (all RRMS) with no history of seizures was included (MS group). Patients' disability was assessed according to the Expanded Disability Status Scale (EDSS). All patients underwent 3-T magnetic resonance imaging (MRI; without corticosteroid use and no relapse within 30 days before the MRI scan) and all MSE patients had a standard 21-channel interictal electroencephalogram (EEG) recording. Additionally, a group of age- and sex-matched healthy subjects (HS group; n = 60) without prior evidence of seizures or psychiatric disorders and normal MRI scans was included. The study was approved by the ethical committees of the State Medical Board of Rhineland-Palatine and University Medicine Greifswald (BB022/19). All subjects provided written informed consent before participation.

MRI acquisition

Individual magnetic resonance images from Mainz were acquired on a 3-T MRI scanner (Magnetom Tim Trio, Siemens, Germany) with a 32-channel head coil. The imaging protocol comprised sagittal three-dimensional (3D) T1-weighted (T1W) magnetization-prepared rapid gradient echo (MP-RAGE) and 3D T2-weighted (T2W) fluid attenuated inversion recovery (FLAIR) sequences with the following acquisition parameters: MP-RAGE: repetition time (TR) = 1900 ms, echo time (TE) = 2.52 ms, inversion time (TI) = 900 ms, flip angle (FA) = 9°, field of view (FoV) = 256×256 mm^2, matrix size = 256×256, slice thickness = 1 mm, voxel size = 1×1×1 mm^3; T2W-FLAIR: TR = 5000 ms, TE = 388 ms, TI = 1800 ms, FoV = 256×256 mm^2, matrix size = 256×256, slice thickness = 1 mm, voxel size = 1×1×1 mm^3.

Images of the participants from Greifswald were acquired on a 3-T Magnetom Verio (Siemens) with a 32-channel head coil. Acquisition parameters were: sagittal 3D T1W MP-RAGE: TR = 1690 ms, TE = 2.52 ms, FoV = 256×256 mm^2, matrix size = 256×256, slice thickness = 1 mm, voxel size = 1×1×1 mm^3; and sagittal 3D T2W FLAIR: TR = 5000 ms, TE = 388 ms, TI = 1800 ms, FA = 8°, FoV = 250×250 mm^2, matrix size = 512×512, slice thickness = 1 mm, voxel size = 0.49×0.49×1 mm^3.

MRI processing

Volumetric segmentation

Cortical surface reconstruction and subsequent cortical, subcortical and hippocampal volumetric parcellations of T1W images were performed with FreeSurfer (version 6.0, http://surfer.nmr.mgh.

harvard.edu/) [23]. To avoid lesion-induced tissue misclassification errors, MRI preprocessing was performed after filling T1 hypointense lesions. For each subject the processing stream consisted of skull stripping, Talairach space transformation, optimization of GM–white matter (WM) and GM–cerebrospinal fluid boundaries, segmentation of subcortical WM and deep GM structures, and surface tessellation with topology correction [23]. Reconstructed cortical surfaces and volumetric parcellations were inspected for accuracy and manually corrected if necessary. Cortical surface was parcellated into 68 anatomical regions according to the Desikan-Killiany atlas [24].

Hippocampal subfields were segmented based on the preliminary T1W subcortical segmentation of the whole hippocampus by applying a Bayesian inference approach and a probabilistic atlas of the hippocampal formation [25]. The left and right hippocampi were each segmented into 12 subfields: parasubiculum, presubiculum, subiculum, cornu ammonis (CA) 1, CA3, CA4, granule cell layer of dentate gyrus, hippocampus–amygdala transition area (HATA), fimbria, molecular layer, hippocampal fissure, and hippocampal tail. FreeSurfer's automated hippocampal subfields segmentation has shown high accuracy and reliability within and across healthy and patient populations [26], and high stability within and across different scanner platforms [27].

Finally, regional volumes of cortical, subcortical GM structures and hippocampal subfields were extracted for subsequent analysis.

Lesion segmentation

For the quantification of lesion volumes we employed the lesion segmentation toolbox (LST; https://www.applied-statistics.de/lst.html) [28], running under statistical parametric mapping (SPM12) software (https://www.fil.ion.ucl.ac.uk/spm/). Automated lesion segmentation was based on the lesion growth algorithm. First, structural T1W images were segmented into GM, WM and cerebrospinal fluid compartments. Afterwards, the 3D FLAIR images were co-registered to the T1W images in order to obtain the lesion belief maps. These maps were thresholded with 20 different initial values to calculate the binary lesion maps. After visual inspection, the threshold of $\kappa = 0.1$ was chosen as the optimal value. Finally, the binary lesion maps were grown along the hyperintense voxels on FLAIR images, resulting in lesion probability maps. To obtain individual lesion volumes of the cortical and subcortical regions, including the hippocampal subfields, the pre-computed lesion probability maps in subject space were superimposed to the parcellation pre-computed on the T1W images.

Network analysis

Network reconstruction

Network analysis was performed via the open-source Brain Connectivity Toolbox (https://sites.google.com/site/bctnet/) [29]. Obtained volumes from cortical, subcortical GM structures, and

hippocampal subfields were embedded into a common connectivity matrix ($N \times N$, where N represents the number of regions; 106×106) for each group (MSE, MS, HS) separately. Each value in the connectivity matrix represents the Pearson correlation between the pairs of regions across group individuals. The connectivity matrices were binarized over a range of density levels ($n = 30$; starting from 0.3 in steps of 0.01). At each density level, the consistency of the network topology was evaluated.

Network topology measures

The following network measures were calculated to describe the topological organization of the networks: transitivity, assortativity, and network resilience. Transitivity, similarly to the clustering coefficient, indicates the number of connections between the neighbouring nodes, but unlike the clustering coefficient, transitivity is not influenced by low-degree nodes [30]. Being the measure of network segregation, transitivity reflects the average level of local connectedness in a network. Assortativity is defined as the preference of a network's node to connect to other nodes that have a similar degree [31]; positive values indicate an assortative network and negative values indicate a disassortative network (i.e., nodes connect preferentially with nodes of different degree). The assortative topology was shown to facilitate synchronization within the networks [32]. The computed network measures were corrected for age, sex and centre.

The resilience of a network relies on a robust and efficient configuration of interregional brain connections and is associated with network stability [33]. To probe the resilience of brain networks, simulated random and targeted attacks were performed based on the transitivity [29, 34]. During random attack, nodes were randomly removed from the network and alterations in network topology (relative size of the remaining largest connected component) were assessed thereafter. The targeted attack performs node removal in a rank order of decreasing nodal betweenness centrality, defined as the number of shortest paths connecting every pair of nodes in the network and crossing through a given node [29]. Low resilience of a network implies increased vulnerability of that particular network to insults [29].

Statistical analysis

The statistical analysis was performed using SPSS software (version 23.0; IBM) and MATLAB R2018b (Mathworks). Group differences in demographic, clinical and MRI-derived variables were assessed with one-way analysis of variance (ANOVA), a Mann–Whitney U-test, a two-sample t-test or Pearson's chi-squared test, as appropriate.

Between-group volumetric variations within the cortical regions, subcortical GM structures and hippocampal subfields were assessed by employing general linear models. All models were adjusted for age, sex, centre and intracranial volume, and corrected

for multiple comparisons (post hoc Bonferroni method). Similarly, general linear models were used to compare the network measures (as dependent variables) among the groups (as independent variable), adjusted for age, sex and centre, and corrected for multiple comparisons. Group differences in network resilience were tested via t-tests, comparing the change in transitivity yielded by each level of random and targeted attack among the MSE, MS and HS groups.

A receiver-operating characteristic (ROC) curve analysis was performed to assess the performance of MRI-derived parameters to distinguish MSE from MS without epilepsy. For each model, area under the curve (AUC) with confidence intervals, sensitivity and specificity were calculated. An AUC greater than 0.5 indicates a good discrimination.

A p-value of less than 0.05 was taken to indicate statistical significance.

RESULTS

Subject characteristics

The groups did not differ either in age or in sex distribution (both $p > 0.05$; Table 1). The MSE and MS patients did not differ in disease duration, but higher EDSS scores were observed in MSE compared to MS (median 3.0 vs. 2.0; $p = 0.02$). Eighteen patients in the MSE group and 53 patients in the MS group were on disease-modifying drug treatment.

Epilepsy characteristics

In the MSE group, the mean age at first seizure presentation was 35.2 ± 12.3 years and the mean elapsed time from MS onset to the

TABLE 1 Demographic, clinical and MRI characteristics of the study groups

	MSE ($n = 30$)	MS ($n = 60$)	HS ($n = 60$)	p value
Female: male (ratio)	21:9 (2.3)	35:25 (1.4)	27:33 (0.8)	0.09[a]
Age, years; mean (SD)	41 (15)	41 (12)	40 (13)	0.86[b]
MS duration, years; mean (SD)	8 (6)	6 (4)	na	0.12[c]
Epilepsy duration, years; mean (SD)	5 (4)	na	na	na
EDSS score, median (range)	3 (0–8)	2 (0–8)	na	**0.02**[d]
Total lesion volume, ml; median (range)	12.8 (0.8–212.0)	8.6 (0.0–90.2)	na	0.09[d]
Total GM lesion volume, ml; median (range)	1.0 (0.0–14.3)	0.6 (0.0–8.2)	na	**0.01**[d]
Total cortical GM lesion volume, ml; median (range)	0.47 (0.04–16.5)	0.12 (0.0–7.6)	na	**0.02**[d]
Global cortical GM volume, ml; mean (SD)	455073.7 (67897.5)	458942.3 (61246.3)	473326.1 (50318.8)	0.27[e]
Global subcortical GM volume, ml; mean (SD)	51719.6 (6410.0)	52448.6 (6558.9)	56090.1 (5278.7)	**0.001**[e]
Global hippocampal volume, ml; mean (SD)	6604.4 (799.2)	6663.6 (762.8)	6961.6 (7391)	0.162
Disease modifying drugs, n (%)				
Beta interferons	2 (6.6)	8 (13.3)		
Glatiramer acetate	4 (13.3)	4 (6.6)		
Fingolimod	6 (20.0)	6 (10.0)		
Dimethyl fumarate	4 (13.3)	18 (30.0)		
Teriflunomide	0 (0.0)	2 (3.3)		
Natalizumab	1 (3.3)	11 (18.3)		
Alemtuzumab	0 (0.0)	2 (3.3)		
Daclizumab	1 (3.3)	0 (0.0)		
Mitoxantron	0 (0.0)	2 (3.3)		
No therapy	12 (40.0)	7 (11.6)		

Abbreviations: EDSS, Expanded Disability Status Scale; GM, grey matter; HS, healthy subjects; MS, multiple sclerosis patients without epilepsy; MSE, multiple sclerosis patients with epilepsy.

[a]Chi-squared test.

[b]One-way analysis of variance.

[c]Independent samples t-test (two-tailed).

[d]Mann–Whitney U-test.

[e]General linear models adjusted for age, sex, centre, and intracranial volume, with Bonferroni correction for multiple comparisons.

Significant p-values are indicated in bold. For all statistical tests the significance level was set to a p-value < 0.05.

first seizure occurrence was 5.5 ± 5.1 years. In none of the cases was seizure the first symptom of MS. The majority of patients experienced focal-onset seizures (84%), impaired consciousness (36%) being the most frequent presentation (Table 2). In more than half of patients (52%), focal to bilateral tonic–clonic progression was confirmed. Twenty-three patients (77%) received antiepileptic drugs, the most commonly prescribed of which was levetiracetam.

Evaluation of regional GM lesion volumes

No significant differences in total T2 lesion volume between the MSE and MS groups were identified but a higher lesion volume within the global GM and cortical GM in the MSE group (both $p < 0.05$) was observed. The MSE group displayed higher lesion volumes within the temporal lobe (left entorhinal, left parahippocampal, left/right fusiform; all $p < 0.05$) and frontal lobe (left pars triangularis; $p = 0.033$) as compared to the MS group (Figure 1). In contrast, higher lesion volumes within the parietal (left/right precuneus; both $p < 0.05$) and occipital (left/right lingual, left/right pericalcarine; all $p < 0.05$) lobes were detected in MS when compared to MSE.

At the subcortical level, between-group comparison revealed significantly higher lesion volumes in the left putamen ($p = 0.019$) and amygdala ($p = 0.037$) in the MSE than the MS group (Figure 2). Lesion volumes within both caudate nuclei were higher in the MS group (both $p < 0.05$).

The MSE group had higher lesion volumes within both hippocampi as compared to the MS group: left hippocampal tail ($p = 0.010$) and HATA ($p = 0.039$), as well as right subiculum ($p = 0.033$) and whole hippocampus ($p = 0.036$; Figure 2).

Regional cortical, subcortical and hippocampal lesion volumes are presented in Table S1.

Evaluation of regional GM volumes

No significant differences in global cortical GM volume among the three groups were attested. In the left hemisphere, the MSE group showed lower volumes of isthmus cingulate (MSE vs. MS, $p = 0.04$; MSE vs. HS, $p = 0.01$) and posterior cingulate (MSE vs. MS, $p < 0.001$; MSE vs. HS, $p < 0.001$ [Figure 3]). The MSE and MS groups both presented lower volumes of left temporal pole compared to the HS group (both $p < 0.05$). In the right hemisphere, the MSE group had lower volumes in several cortical regions as compared to the MS and HS groups: entorhinal (MSE vs. MS, $p = 0.006$; MSE vs. HS, $p = 0.007$), parahippocampal (MSE vs. MS, $p = 0.01$; MSE vs. HS, $p = 0.001$), isthmus cingulate (MSE vs. MS, $p = 0.02$; MSE vs. HS, $p = 0.001$), and posterior cingulate (MSE vs. MS, $p = 0.006$; MSE vs. HS, $p < 0.001$). Additionally, lower volumes of the right fusiform and lingual cortices were detected in the MSE compared to the HS group (both $p < 0.05$).

On a subcortical level, both MSE and MS patients had lower left caudate and putamen volumes as compared to HS (all $p < 0.05$; Figure 3). In the right hemisphere, both MSE and MS patients had lower thalamus, caudate and putamen volumes as compared to HS (all $p < 0.05$). Lower volumes of both globi pallidi were observed in MSE compared to MS patients (both $p < 0.05$).

Hippocampal subfield analysis revealed lower volumes of the left hippocampal tail and presubiculum in both the MSE and MS groups as compared to the HS group (both $p < 0.05$; Figure 3). In the MSE group, left fimbria volume was lower compared to the MS and HS groups (all $p < 0.05$). Within the contralateral hemisphere, both the MSE and MS groups had lower presubiculum volume as compared to the HS group (both $p < 0.05$). Right fimbria volume was lower in the MS compared to the HS group ($p = 0.027$).

Regional cortical, subcortical and hippocampal volumes are presented in Table S2.

Network topology and resilience

The network architecture was characterized by higher transitivity ($F_{2,87} = 4.9$, $p = 0.009$) and assortativity ($F_{2,87} = 98.4$, $p < 0.001$) in the MSE compared to the MS and HS groups (Figure 4a).

Upon random attack, resilience of the GM networks was comparable among the three groups in all proportions of the removed nodes (all $p > 0.05$; Figure 4b). In contrast, the response of GM

TABLE 2 Characteristics of seizures in multiple sclerosis patients with epilepsy

Seizure type, n (%)	Seizure semiology, n (%)	Impairment of consciousness during seizure, n (%)	Focal to bilateral tonic–clonic, n (%)	Antiepileptic drugs, n (%)
Focal – 25 (84)	Focal unaware – 9 (36) Focal motor – 6 (24) Focal sensory – 3 (12) Focal sensory-motor – 7 (28)	Impaired – 16 (64) Preserved – 9 (36)	Present – 18 (52) Absent – 12 (48)	LEV – 9 (36) LTG – 3 (12) LCS – 1 (4) PMP – 1 (4) CBZ – 1 (4) Combination – 4 (16) None – 6 (24)
Generalized – 5 (16%)	Motor – 5 (100)	Impaired – 5 (100)	–	LEV – 4 (80) None – 1 (20)

Abbreviations: CBZ, carbamazepine; LCS, lacosamide; LEV, levetiracetam; LTG, lamotrigine; PMP, perampanel.
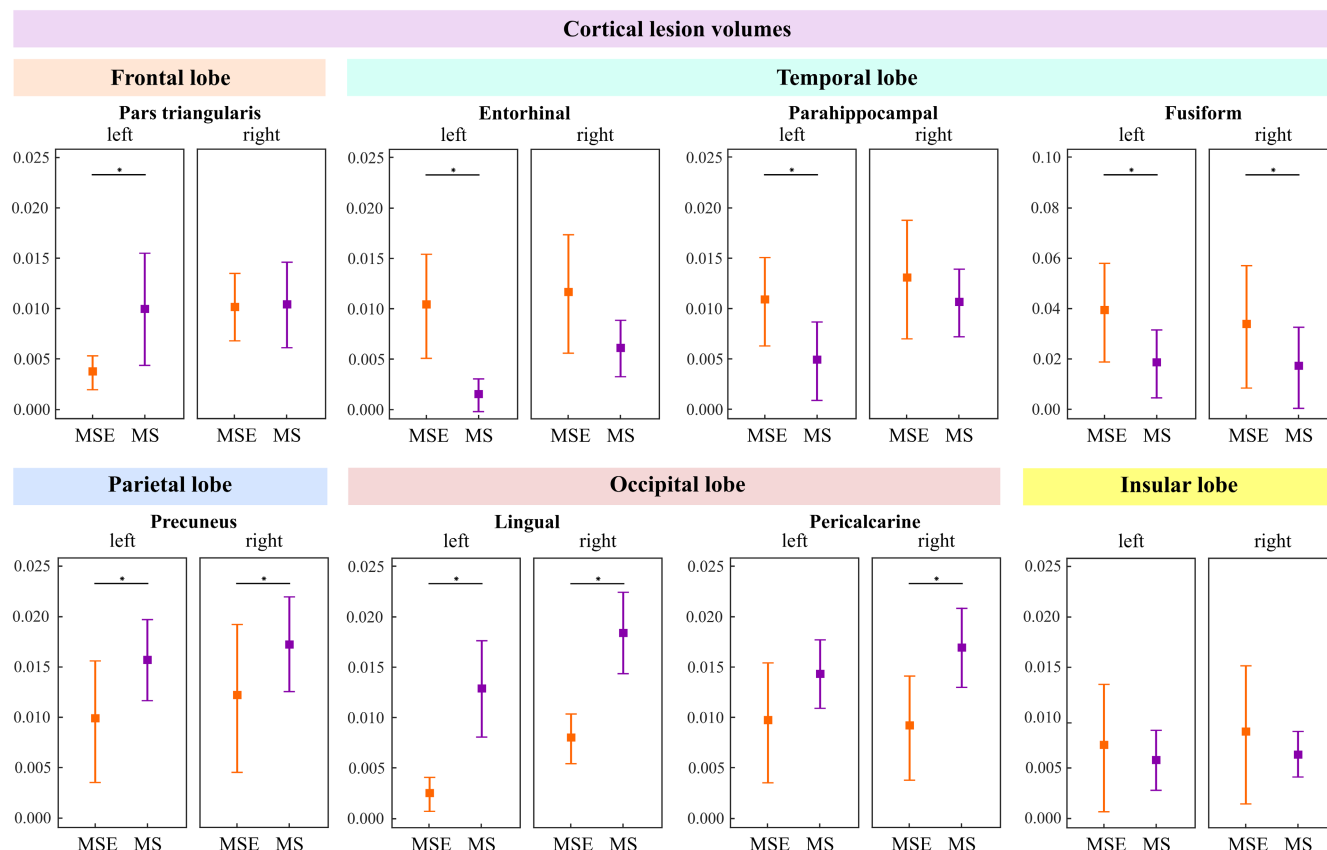
FIGURE 1 Lesion volumes across cortical regions. Median values (with 95% confidence intervals) displaying the differences in lesion volumes within cortical regions between the multiple sclerosis patients with epilepsy (MSE) and multiple sclerosis (MS) patients without epilepsy; *$p < 0.05$ [Colour figure can be viewed at wileyonlinelibrary.com]

networks to targeted attack significantly differed among the groups at several fractions of the removed nodes. The MSE group exhibited the lowest resilience across a large range of steps (node removals), presenting significant network breakdowns at smaller factions of removed nodes as compared to the MS and HS groups (all $p < 0.05$).

ROC curve analysis

In the first model, we evaluated which variables among total lesion volume, global GM or global hippocampal volumes could discriminate MS patients with and without epilepsy. Total lesion volume performed best in discriminating between MSE and MS patients, with an AUC of 0.76 (0.61–0.91), whereas global hippocampal volume and global GM volume yielded similar AUCs of 0.58 (0.43–0.73) and 0.53 (0.39–0.67), respectively (Figure 5; Table S3). Pairwise comparison revealed that the AUC of total brain lesion volume was significantly different from the AUC of global hippocampal and global GM volumes (both $p < 0.05$). In the second model, we investigated exactly in which brain compartment (cortical, subcortical or hippocampal) lesion volume could better discriminate between the MSE and MS patients. We found that total hippocampal lesion volume achieved the highest accuracy, with an AUC of 0.80 (0.67–0.91), followed by total cortical lesion volume, with an AUC of 0.72 (0.56–0.87) and

total subcortical lesion volume, with an AUC of 0.71 (0.57–0.86 [Figure 5]). At a hippocampal regional level, lesion volume of the subiculum (AUC = 0.74; CI 0.61–0.84) yielded the highest accuracy in discriminating between MSE and MS patients (Table S4).

DISCUSSION

Aiming to identify the MRI-derived correlates of epilepsy occurrence in MS patients, we found that increased lesion volumes and GM tissue loss, particularly within the hippocampal, cortical (temporal and parietal) and subcortical (amygdala) compartments, were associated with emergence of epilepsy in MS. Hippocampal subfield lesion volumes, followed by cortical lesion volumes, were able to distinguish MS patients with epilepsy from those without more accurately. Highly segregated and vulnerable network architecture in MSE patients was consistent with a more compromised GM integrity in this group.

Regional GM lesions

Inflammatory damage within the cortical GM is considered to be an important contributor to seizure and epilepsy occurrence in MS
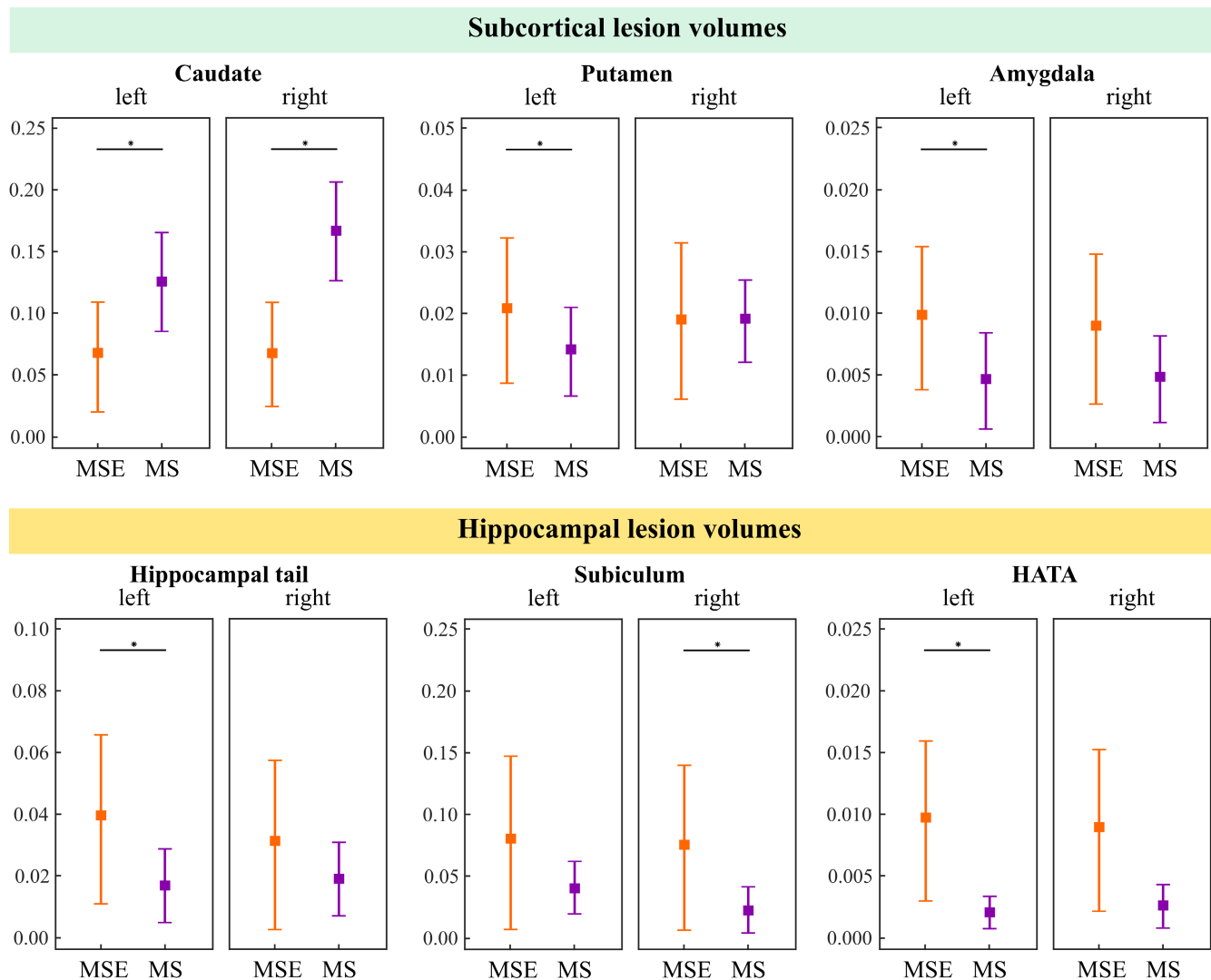
FIGURE 2 Lesion volumes across subcortical regions and hippocampal subfields. Median values (with 95% confidence intervals) of lesion volumes within subcortical grey matter structures and hippocampal subfields between the multiple sclerosis patients with epilepsy (MSE) and multiple sclerosis (MS) patients without epilepsy; *$p < 0.05$. HATA, hippocampus–amygdala transition area [Colour figure can be viewed at wileyonlinelibrary.com]

patients [5, 6]. MS patients with concomitant epilepsy have a higher lesion burden within the cortical GM [7] and tend to accumulate new cortical lesions over time [6]. Concordantly, the present analysis evidenced that MSE had higher lesion volumes within the global and cortical GM, which were unevenly distributed across the cortical mantle, with higher lesion load in the mesial temporal lobe and lower lesion load in the parietal and occipital lobe areas. We found, in particular, that the hippocampus, parahippocampal, entorhinal and fusiform cortices were characterized by higher lesion volumes in MSE than in MS patients. This suggests that, in addition to GM lesion load, the topographical location of the lesions may be a key factor predisposing to seizure occurrence. The relevance of temporal lobe damage for seizure occurrence has been postulated by previous studies. For instance, Calabrese et al. reported that, among GM structures, the hippocampal formation is most heavily affected by lesions in RRMS patients with epilepsy compared to patients without epilepsy, followed by the temporal, cingulate and insular cortices

[9]. This pattern of mesial temporal lobe damage is consistent with our findings and highlights the role of the hippocampus and nearby cortical areas in seizure susceptibility.

Compared with previous studies, we quantified the compartmentalized distribution of lesion volumes across the hippocampal subfields and detected higher lesion volumes in the subiculum, hippocampal tail and HATA of the MSE patients. In temporal lobe epilepsy, the cell populations of the hippocampal subfields differ in their vulnerability to damage and excitability properties [35], with the subiculum being considered to be an important site of icto- and epileptogenesis [36]. Higher hippocampal lesion load in MSE patients was clinically reflected in the higher frequency of focal-unaware seizures, the phenotype closely associated with temporal lobe epilepsy and that most frequently observed in our study population. MSE patients also experienced extratemporal lobe seizures (e.g., focal motor or sensory onset seizures), but these cortical regions were not marked by higher lesion volumes compared to MS patients.
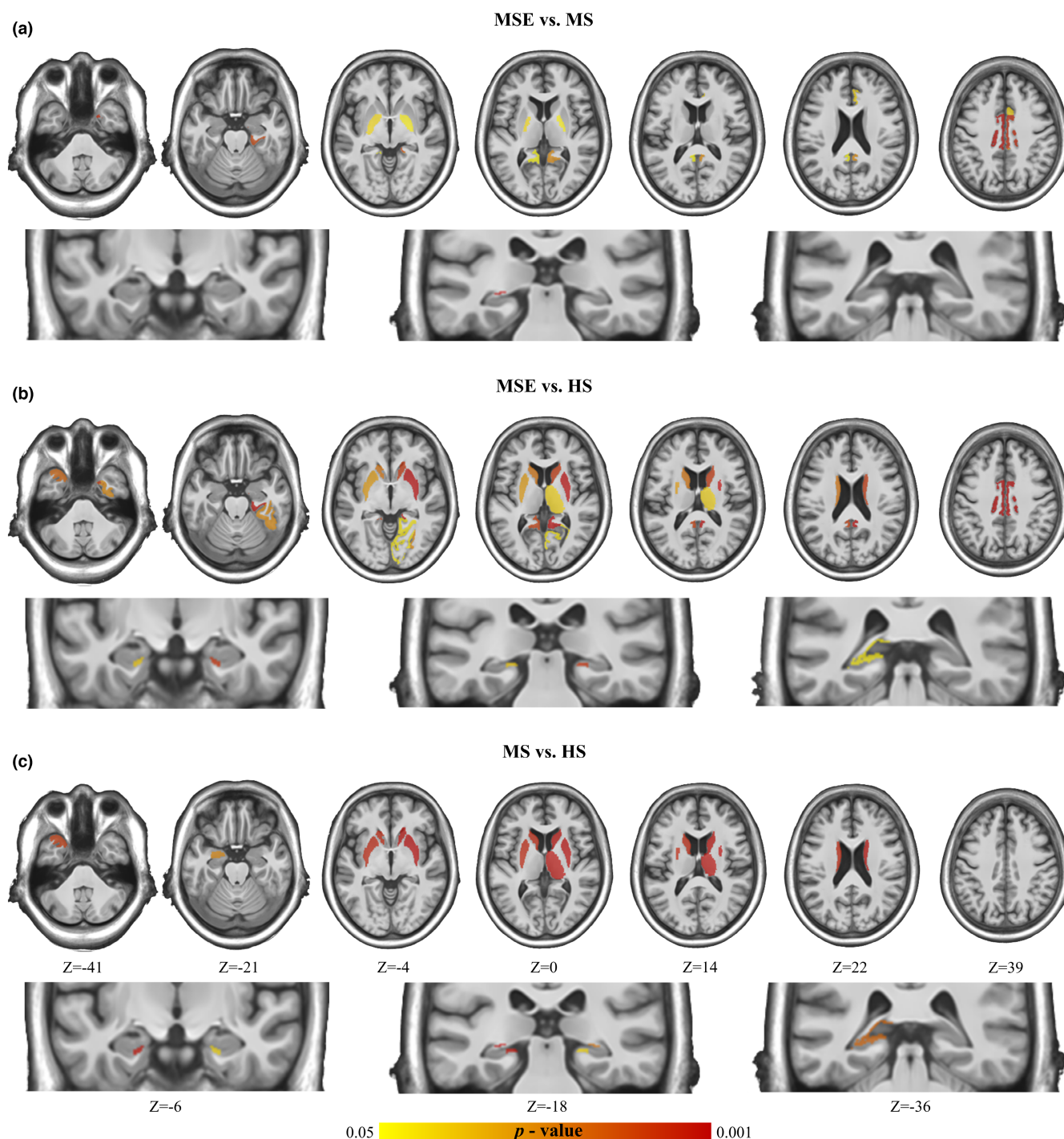
FIGURE 3 Between-group differences in regional grey matter volumes. Axial and coronal slices (with corresponding MNI coordinates) displaying which cortical and subcortical grey matter volumes and hippocampal subfield volumes differ between the multiple sclerosis patients with epilepsy (MSE), multiple sclerosis (MS) patients without epilepsy, and healthy subjects (HS) [Colour figure can be viewed at wileyonlinelibrary.com]

Regional GM volumes

Our results show that GM integrity of MSE patients was most severely affected compared to MS patients and HS with volume reductions detected mainly within the mesiotemporal and parietal cortices. This spatial pattern of atrophy might in part explain the higher frequency of focal-unaware and focal-onset sensory seizures in MSE patients. A recent study pointed out the predominant involvement of the temporal lobe regions, with cortical thickness of the fusiform gyrus being associated with seizure appearance [9]. Selective loss of GABA interneurons in cortical layers IV and VI was proposed as the underlying mechanism of temporal cortical atrophy and hyperexcitability [5]. This selective loss of inhibitory neurons was related to type I cortical lesions (leukocortical lesions), which
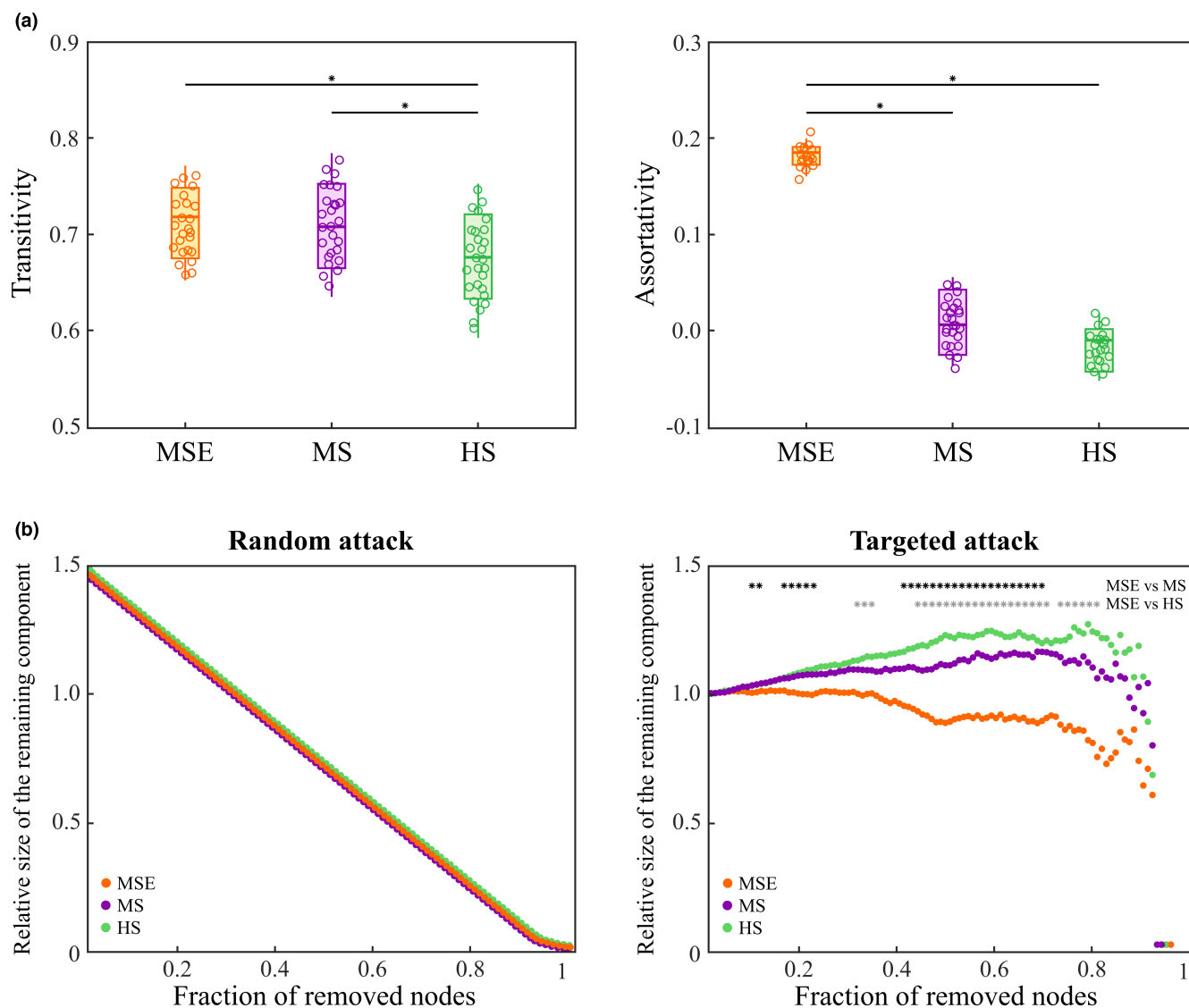
FIGURE 4 Network topology measures and network resilience. (a) Boxplots displaying the differences in transitivity and assortativity between the multiple sclerosis patients with epilepsy (MSE), multiple sclerosis patients (MS) without epilepsy, and healthy subjects (HS). (b) Alterations in the relative size of the largest component of the network depending on the fraction of random and targeted node removal. Asterisks indicate at which fractions the difference in the size of the largest remaining components between the groups is significant; *$p < 0.05$ [Colour figure can be viewed at wileyonlinelibrary.com]

could be the source of inflammatory cells responsible for neuronal injury [5].

Overall, our and other available data suggest that MSE patients display more extensive and pronounced cortical atrophy, which, however, does not fully explain the complex interrelations between seizure generation and GM tissue loss. Does concomitant epilepsy in MS cause additional GM loss or does epilepsy emerge in MS patients with a more advanced cortical atrophy? One hint could be that in some patients with temporal lobe epilepsy, cortical regions (e.g., entorhinal or piriform) with neuronal loss are the sites of seizure generation [37], indicating that epilepsy in MS patients might emerge from more severely injured cortical areas. Given that both MS and MSE patients have higher cortical volume loss compared to HS, additional damage such as lesion load, lesion type, and topography are

important factors for initiation and maintenance of epileptogenic processes.

Both MS and temporal lobe epilepsy are characterized by selective regional loss of hippocampal tissue [38, 39], which was also confirmed in our data for MSE and MS patients. It is widely accepted that temporal lobe seizures due to hippocampal sclerosis originate from the atrophied CA1 and CA4 subfields [35]. We did not find any volumetric differences in these subfields in MSE patients as compared to MS patients, suggesting potentially different mechanisms underlying neuronal cell loss and hyperexcitability in MS and hippocampal sclerosis. Instead, the volumes of bilateral fimbria in our study were found to be greater in MSE as compared to MS patients. This unexpected finding could be explained either by larger extra-axonal spaces and loose axonal arrangement evidenced in epilepsy
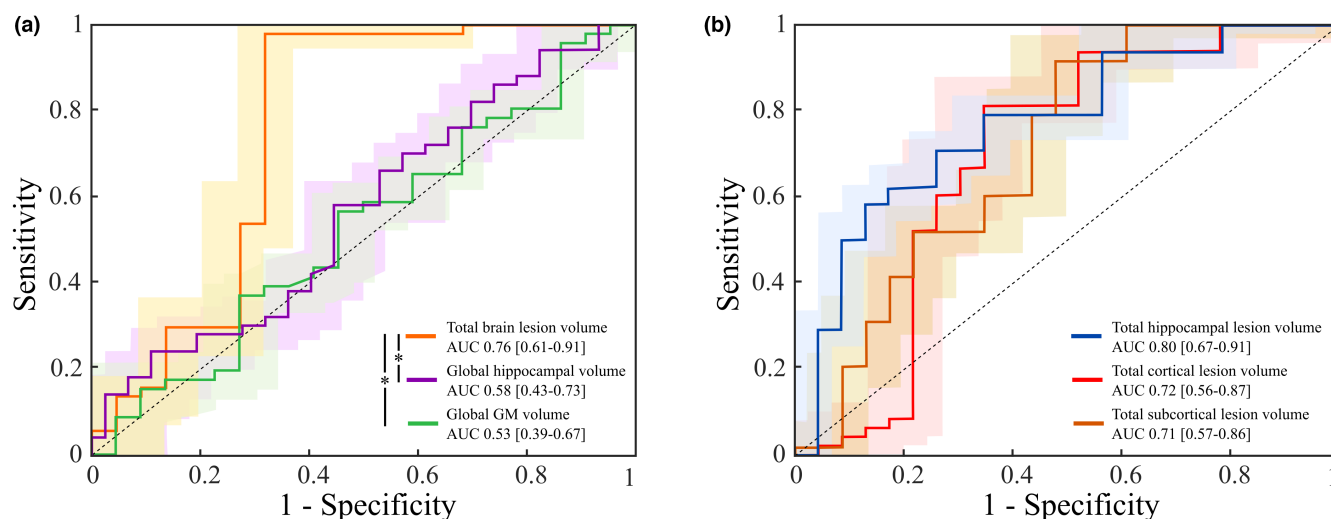
FIGURE 5 Receiver operating characteristic analysis. Area under the ROC curve (AUC) measured the accuracy of total brain lesion volume, global hippocampal volume, and global grey matter volume (a) and total cortical lesion volume, total subcortical lesion volume, and total hippocampal lesion volume (b) in discriminating the multiple sclerosis patients with epilepsy (MSE) from multiple sclerosis (MS) patients without epilepsy. The shadowed areas represent the 95% confidence intervals. In the legend, comparison between the AUCs is shown; *p < 0.05 [Colour figure can be viewed at wileyonlinelibrary.com]

patients with hippocampal sclerosis [40], by higher lesion load (relative to MS patients) or by the limited sample size of MSE.

Network topology and vulnerability

Both MS and epilepsy are associated with network remodelling, with a shift towards a more segregated topology [41]. Since increased network transitivity is observed in both MS [42] and epilepsy [18, 43], an additional effect of seizures (apart from that caused by MS pathology) on network topology in MSE might be expected. Indeed, MSE patients displayed a slightly higher transitivity as compared to MS patients. Increased transitivity in MSE and MS patients might be interpreted as an adaptive response of brain networks to tissue damage directed to maintain network efficiency through enhanced local connectivity [10]. Increased network segregation was also confirmed by high assortativity in both MSE and MS patients, a property that implies an increased tendency of network nodes to connect to other nodes with a similar degree. Strikingly assortative architecture of GM networks in MSE might serve as an underlying structural scaffold for seizure susceptibility as high assortativity values were associated with network synchronizability and the transition to an ictal state in epilepsy patients [44]. However, it remains to be elucidated in future studies whether this is merely a response of the networks to an already hyperexcitable state of the lesioned GM tissue or whether this network architecture promotes a more epileptogenic environment.

Resilience is defined as the ability of brain networks to preserve appropriate network performance despite the presence of structural damage or functional insults [45]. Our findings revealed that, upon targeted attack, the network topology in MSE patients was highly vulnerable to simulated removal of network nodes key for information flows. This indicates that pathological attacks to the most interconnected nodes (network hubs) will be followed by a disproportionately greater impact on communicability than attacks on non-hub regions. The notably reduced network resilience in MSE patients might stem from the cumulative effect of decreased resilience due to MS pathology [46] on one side and decreased resilience due to epileptic seizures [43] on the other. As both MS and epilepsy tend to affect network hubs, it can be postulated that MSE patients might have fewer parallel or alternative pathways to maintain network integrity [47].

MRI predictors of epilepsy in MS

According to our findings, hippocampal (particularly subicular) and cortical lesion volumes but not the GM volumes achieved the highest classification performance in distinguishing between MS patients with and without epilepsy. New cortical lesions, as well as volume of cortical lesions and hippocampal lesions, were previously identified as independent predictors of epilepsy occurrence in RRMS patients [6, 9]. Currently, the degree of contribution of inflammatory lesions and neurodegenerative tissue loss to seizure occurrence in MS is largely unknown. According to one point of view, the risk of seizures is higher during the first years after MS onset given the high occurrence of seizures during relapses [48] and cortical hyperexcitability in RRMS patients [49], thus prioritizing the neuroinflammatory basis of seizure precipitation. An alternative point of view places emphasis on neurodegenerative priming, as seizure recurrence is higher in SPMS than in RRMS patients [50] and the risk of seizures increases with advanced disease and disability [4].

Study limitations

Despite the relatively small sample size of the MSE patients, which was similar to that in previous studies [6, 9], the obtained findings were consistent with these reported data. To minimize the effects of MRI scanners on the accuracy of our results, we included the type of scanner as a confounding factor in the statistical analysis. In addition, brain segmentation performed in FreeSurfer shows high reliability across different scanner platforms [27]. The segmentation of brain lesions based on 3-T T1W and FLAIR sequences is not as sensitive as other more advanced techniques (e.g., 7-T MRI) in detection of cortical lesions, hence, some cortical lesions could be missed in MSE and MS patients. Nevertheless, higher cortical lesion load was obvious in MSE compared to MS patients. Due to the cross-sectional setting of this study and the inclusion of mainly RRMS patients, we cannot address some of the questions related to the MSE patients, for example, further clinical course of the disease and epilepsy, longitudinal alterations in brain morphometric measures and network dynamics, and so on.

CONCLUSIONS

Lesion volume and altered integrity within distinct GM compartments are associated with an increased susceptibility of seizure occurrence in MS. Among others, hippocampal and temporal cortical damage are particularly relevant for epilepsy appearance in MS patients. Network responses – topology reorganization along with higher network vulnerability – might additionally facilitate seizure generation. These findings provide new insights into the structural and network alterations linked to seizure occurrence in MS patients that might be valuable for early identification of MS patients prone to developing epilepsy.

AUTHOR CONTRIBUTIONS

Gabriel Gonzalez-Escamilla: Data curation (equal); methodology (equal); software (equal); visualization (equal); writing – original draft (equal); writing – review and editing (equal). **Yaroslav Winter:** Data curation (equal); writing – review and editing (equal). **Nico Melzer:** Writing – review and editing (equal). **Felix Luessi:** Data curation (equal); writing – review and editing (equal). **Angela Radetz:** Data curation (equal); writing – review and editing (equal). **Vinzenz Fleischer:** Data curation (equal); writing – review and editing (equal). **Stanislav Alexandru Groppa:** Writing – review and editing (equal). **Michael Kirsch:** Writing – review and editing (equal). **Stefan Bittner:** Data curation (equal); writing – review and editing (equal). **Frauke Zipp:** Data curation (equal); writing – review and editing (equal). **Muthuraman Muthuraman:** Data curation (equal); writing – review and editing (equal). **Sven G. Meuth:** Conceptualization (equal); writing – review and editing (equal). **Matthias Grothe:** Conceptualization (equal); data curation (equal); methodology (equal); resources (equal); supervision (equal); writing – review and editing (equal). **Sergiu Groppa:** Conceptualization (equal); data curation (equal); methodology (equal); resources (equal); supervision (equal); writing – review and editing (equal).

CONFLICT OF INTEREST
None.

DATA AVAILABILITY STATEMENT
Data supporting the findings of this study are available from the corresponding author upon reasonable request.

ORCID
Dumitru Ciolac https://orcid.org/0000-0003-1243-313X
Gabriel Gonzalez-Escamilla https://orcid.org/0000-0002-7209-1736
Stefan Bittner https://orcid.org/0000-0003-2179-3655
Sergiu Groppa https://orcid.org/0000-0002-2551-5655

REFERENCES
1. Langenbruch L, Krämer J, Güler S, et al. Seizures and epilepsy in multiple sclerosis: epidemiology and prognosis in a large tertiary referral center. *J Neurol.* 2019;266(7):1789-1795.
2. Neuß F, von Podewils F, Wang ZI, Süße M, Zettl UK, Grothe M. Epileptic seizures in multiple sclerosis: prevalence, competing causes and diagnostic accuracy. *J Neurol.* 2020;1-7:1721-1727.
3. Eriksson M, Ben-Menachem E, Andersen O. Epileptic seizures, cranial neuralgias and paroxysmal symptoms in remitting and progressive multiple sclerosis. *Mult Scler J.* 2002;8(6):495-499.
4. Burman J, Zelano J. Epilepsy in multiple sclerosis: a nationwide population-based register study. *Neurology.* 2017;89(24):2462-2468.
5. Nicholas R, Magliozzi R, Campbell G, Mahad D, Reynolds R. Temporal lobe cortical pathology and inhibitory GABA interneuron cell loss are associated with seizures in multiple sclerosis. *Mult Scler J.* 2016;22(1):25-35.
6. Calabrese M, Grossi P, Favaretto A, et al. Cortical pathology in multiple sclerosis patients with epilepsy: a 3 year longitudinal study. *J Neurol Neurosurg Psychiatry.* 2012;83(1):49-54.
7. Calabrese M, De Stefano N, Atzori M, et al. Extensive cortical inflammation is associated with epilepsy in multiple sclerosis. *J Neurol.* 2008;255(4):581-586.
8. Muthuraman M, Fleischer V, Kroth J, et al. Covarying patterns of white matter lesions and cortical atrophy predict progression in early MS. *Neurol Neuroimmunol Neuroinflamm.* 2020;7(3):e681.
9. Calabrese M, Castellaro M, Bertoldo A, et al. Epilepsy in multiple sclerosis: the role of temporal lobe damage. *Mult Scler J.* 2017;23(3):473-482.
10. Fleischer V, Groger A, Koirala N, et al. Increased structural white and grey matter network connectivity compensates for functional decline in early multiple sclerosis. *Mult Scler.* 2017;23(3):432-441.
11. Radetz A, Koirala N, Krämer J, et al. Gray matter integrity predicts white matter network reorganization in multiple sclerosis. *Hum Brain Mapp.* 2020;41(4):917-927.

12. Muthuraman M, Fleischer V, Kolber P, Luessi F, Zipp F, Groppa S. Structural brain network characteristics can differentiate CIS from early RRMS. *Front Neurosci.* 2016;10:14.

13. Ciolac D, Luessi F, Gonzalez-Escamilla G, et al. Selective brain network and cellular responses upon dimethyl fumarate immunomodulation in multiple sclerosis. *Front Immunol.* 2019;10:1779.

14. Chiosa V, Groppa SA, Ciolac D, et al. Breakdown of thalamo-cortical connectivity precedes spike generation in focal epilepsies. *Brain Connect.* 2017;7(5):309-320.

15. Groppa S, Moeller F, Siebner H, et al. White matter microstructural changes of thalamocortical networks in photosensitivity and idiopathic generalized epilepsy. *Epilepsia.* 2012;53(4):668-676.

16. Groppa S, Siebner HR, Kurth C, Stephani U, Siniatchkin M. Abnormal response of motor cortex to photic stimulation in idiopathic generalized epilepsy. *Epilepsia.* 2008;49(12):2022-2029.

17. Fleischer V, Radetz A, Ciolac D, et al. Graph theoretical framework of brain networks in multiple sclerosis: a review of concepts. *Neuroscience.* 2019;403:35-53.

18. Chiosa V, Ciolac D, Groppa S, et al. Large-scale network architecture and associated structural cortico-subcortical abnormalities in patients with sleep/awake-related seizures. *Sleep.* 2019;42:zsz006.

19. Polman CH, Reingold SC, Banwell B, et al. Diagnostic criteria for multiple sclerosis: 2010 revisions to the McDonald criteria. *Ann Neurol.* 2011;69(2):292-302.

20. Fisher RS, Acevedo C, Arzimanoglou A, et al. ILAE official report: a practical clinical definition of epilepsy. *Epilepsia.* 2014;55(4):475-482.

21. Scheffer IE, Berkovic S, Capovilla G, et al. ILAE classification of the epilepsies: position paper of the ILAE commission for classification and terminology. *Epilepsia.* 2017;58(4):512-521.

22. Fisher RS, Cross JH, French JA, et al. Operational classification of seizure types by the international league against epilepsy: position paper of the ILAE commission for classification and terminology. *Epilepsia.* 2017;58(4):522-530.

23. Fischl B. FreeSurfer. *Neuroimage.* 2012;62(2):774-781.

24. Desikan RS, Ségonne F, Fischl B, et al. An automated labeling system for subdividing the human cerebral cortex on MRI scans into gyral based regions of interest. *Neuroimage.* 2006;31(3):968-980.

25. Iglesias JE, Augustinack JC, Nguyen K, et al. A computational atlas of the hippocampal formation using ex vivo, ultra-high resolution MRI: application to adaptive segmentation of in vivo MRI. *Neuroimage.* 2015;115:117-137.

26. Whelan CD, Hibar DP, van Velzen LS, et al. Heritability and reliability of automatically segmented human hippocampal formation subregions. *Neuroimage.* 2016;128:125-137.

27. Brown EM, Pierce ME, Clark DC, et al. Test-retest reliability of FreeSurfer automated hippocampal subfield segmentation within and across scanners. *Neuroimage.* 2020;210:116563.

28. Schmidt P, Gaser C, Arsic M, et al. An automated tool for detection of FLAIR-hyperintense white-matter lesions in multiple sclerosis. *Neuroimage.* 2012;59(4):3774-3783.

29. Rubinov M, Sporns O. Complex network measures of brain connectivity: uses and interpretations. *Neuroimage.* 2010;52(3):1059-1069.

30. Newman ME. The structure and function of complex networks. *SIAM Rev.* 2003;45(2):167-256.

31. Newman ME. Assortative mixing in networks. *Phys Rev Lett.* 2002;89(20):208701.

32. di Bernardo M, Garofalo F, Sorrentino F. Effects of degree correlation on the synchronization of networks of oscillators. *Int J Bifurc Chaos.* 2007;17(10):3499-3506.

33. Bullmore E, Sporns O. The economy of brain network organization. *Nat Rev Neurosci.* 2012;13(5):336-349.

34. Kaiser M, Martin R, Andras P, Young MP. Simulation of robustness against lesions of cortical networks. *Eur J Neurosci.* 2007;25(10):3185-3192.

35. Wozny C, Knopp A, Lehmann TN, Heinemann U, Behr J. The subiculum: a potential site of ictogenesis in human temporal lobe epilepsy. *Epilepsia.* 2005;46:17-21.

36. Stafstrom CE. The role of the subiculum in epilepsy and epileptogenesis. *Epilepsy Curr.* 2005;5(4):121-129.

37. Vismer MS, Forcelli PA, Skopin MD, Gale K, Koubeissi MZ. The piriform, perirhinal, and entorhinal cortex in seizure generation. *Front Neural Circuits.* 2015;9:27.

38. Planche V, Koubiyr I, Romero JE, et al. Regional hippocampal vulnerability in early multiple sclerosis: dynamic pathological spreading from dentate gyrus to CA 1. *Hum Brain Mapp.* 2018;39(4):1814-1824.

39. Schoene-Bake JC, Keller SS, Niehusmann P, et al. In vivo mapping of hippocampal subfields in mesial temporal lobe epilepsy: relation to histopathology. *Hum Brain Mapp.* 2014;35(9):4718-4728.

40. Concha L, Livy DJ, Beaulieu C, Wheatley BM, Gross DW. In vivo diffusion tensor imaging and histopathology of the fimbria-fornix in temporal lobe epilepsy. *J Neurosci.* 2010;30(3):996-1002.

41. Gonzalez-Escamilla G, Ciolac D, De Santis S, et al. Gray matter network reorganization in multiple sclerosis from 7-Tesla and 3-Tesla MRI data. *Ann Clin Transl Neurol.* 2020;7(4):543-553.

42. Fleischer V, Koirala N, Droby A, et al. Longitudinal cortical network reorganization in early relapsing–remitting multiple sclerosis. *Ther Adv Neurol Disord.* 2019;12:1756286419838673.

43. Sone D, Matsuda H, Ota M, et al. Impaired cerebral blood flow networks in temporal lobe epilepsy with hippocampal sclerosis: a graph theoretical approach. *Epilepsy Behav.* 2016;62:239-245.

44. Bialonski S, Lehnertz K. Assortative mixing in functional brain networks during epileptic seizures. *Chaos.* 2013;23(3):33139.

45. Gonzalez-Escamilla G, Muthuraman M, Chirumamilla VC, Vogt J, Groppa S. Brain networks reorganization during maturation and healthy aging-emphases for resilience. *Front Psych.* 2018;9:601.

46. Llufriu S, Rocca MA, Pagani E, et al. Hippocampal-related memory network in multiple sclerosis: a structural connectivity analysis. *Mult Scler J.* 2019;25(6):801-810.

47. Bernhardt BC, Chen Z, He Y, Evans AC, Bernasconi N. Graph-theoretical analysis reveals disrupted small-world organization of cortical thickness correlation networks in temporal lobe epilepsy. *Cereb Cortex.* 2011;21(9):2147-2157.

48. Sponsler JL, Kendrick-Adey AC. Seizures as a manifestation of multiple sclerosis. *Epileptic Disord.* 2011;13(4):401-410.

49. Caramia MD, Palmieri MG, Desiato MT, et al. Brain excitability changes in the relapsing and remitting phases of multiple sclerosis: a study with transcranial magnetic stimulation. *Clin Neurophysiol.* 2004;115(4):956-965.

50. Mahamud Z, Burman J, Zelano J. Risk of epilepsy after a single seizure in multiple sclerosis. *Eur J Neurol.* 2018;25(6):854-860.

SUPPORTING INFORMATION

Additional supporting information may be found in the online version of the article at the publisher's website.

Table S1-S4

How to cite this article: Ciolac D, Gonzalez-Escamilla G, Winter Y, et al. Altered grey matter integrity and network vulnerability relate to epilepsy occurrence in patients with multiple sclerosis. *Eur J Neurol.* 2022;29:2309-2320. doi: [10.1111/ene.15405](10.1111/ene.15405)